Assessing a Dysplastic Cerebellar Gangliocytoma (Lhermitte-Duclos Disease) with 7T MR Imaging

Christoph Moenninghoff, MD[1, 2]
Oliver Kraff, MSc[1, 2]
Marc Schlamann, MD[1, 2]
Mark E. Ladd, PhD[1, 2]
Zaza Katsarava, MD[3]
Elke R. Gizewski, MD[1, 2]

Lhermitte-Duclos disease (LDD; dysplastic cerebellar gangliocytoma) is a rare hamartomatous lesion of the cerebellar cortex and this was first described in 1920. LDD is considered to be part of the autosomal-dominant phacomatosis and cancer syndrome Cowden disease (CS). We examined the brain of a 46-year-old man, who displayed the manifestations of CS, with 7 Tesla (T) and 1.5T MRI and 1.5T MR spectroscopy (^{1}H-MRS). We discuss the possible benefits of employing ultrahigh-field MRI for making the diagnosis of this rare lesion.

Index terms:
Lhermitte-Duclos disease
7 Tesla
Magnetic resonance (MR)
Dysplastic cerebellar gangliocytoma
Susceptibility-weighted imaging

DOI:10.3348/kjr.2010.11.2.244

Korean J Radiol 2010;11:244-248
Received February 2, 2009; accepted after revision September 18, 2009.

[1]Department of Diagnostic and Interventional Radiology and Neuroradiology, University Hospital Essen, Germany; [2]Erwin L. Hahn Institute for Magnetic Resonance Imaging, University Duisburg-Essen, Germany; [3]Department of Neurology, University Hospital Essen, Germany

Address reprint requests to:
Christoph Moenninghoff, MD, Department of Diagnostic and Interventional Radiology and Neuroradiology, University Hospital Essen, Hufelandstra β e 55, D-45147 Essen, Germany.
Tel. (49201) 723-84549
Fax. (49201) 723-1563
e-mail: ch.moenninghoff@uk-essen.de

Lhermitte-Duclos disease (LDD; dysplastic gangliocytoma of the cerebellum) is a rare cerebellar hamartoma, and this was first described by Lhermitte and Duclos in 1920 (1). Since 1991 LDD has been considered to be part of Cowden disease (CS), which is an autosomal-dominant phacomatosis and cancer syndrome, and LDD is characterized by multiple hamartomas and a high risk of breast, thyroid and endometrial carcinoma (2). This 'multiple hamartoma-neoplasia syndrome' is associated with mutations of the *PTEN* gene. Over 225 cases of LDD have currently been reported in medical literature (3).

7T MRI whole-body scanners are currently being evaluated for possible clinical applications. Their higher magnetic field strength allows improving the spatial resolution and reducing the scan time without sacrificing the signal-to-noise ratio (SNR) and the contrast-to-noise ratio (CNR), as compared to lower field strength MRI. In this report we assess the usefulness of the T2*, T2, and susceptibility-weighted imaging (SWI) at 7T, as compared with routine MR imaging at 1.5T, in a male patient with genetically proven LDD.

CASE REPORT

A 46-year-old Caucasian man presented with a 10-year history of mild gait ataxia and undirected vertigo after fast head movements. The patient had suffered from disturbed urination for the previous 25 years. He had a past medical history of resection of a thyroid adenoma and also for benign polyposis of the sigmoid colon. At the age of 41 years, a seborrheic keratosis was excised from his right ear. The patient had no familial history of LDD or hereditary disease. Physical inspection revealed megalocephaly, congenital facial asymmetry and left thenar aplasia. At the latest presentation, the neurological examination showed minimal intention tremor, gait ataxia without visual compensation, an undirected imbalance on Romberg's test and bradydiadochokinesia.

With approval of the local ethic committee and with the patient's informed written consent, MRI examinations of the brain were performed on a 1.5T scanner (Avanto,

Siemens Medical Solutions, Erlangen, Germany) in combination with using a vendor supplied 12-channel receive-only head coil and then MRI examinations of the brain were done on a 7T scanner (Magnetom 7T, Siemens Medical Solutions, Erlangen, Germany) in combination with an 8-channel transmit-and-receive head coil (Rapid Biomed, Wuerzburg, Germany). The gradient-echo and turbo spin echo sequences were performed to obtain the axial proton density (PD), T2, T2* and susceptibility weighted images (SWI), which were optimized for each field strength (Table 1).

In addition, proton (^{1}H) MR spectroscopy (MRS) was performed at 1.5T. The spectroscopic data was acquired from the patient's cerebellar lesion using a single-voxel, point-resolved technique (TE = 135 ms; TR = 1500 ms). The resulting prominent resonances representing choline (Cho), creatine (Cr) and N-acetylaspartate (NAA) within the lesion were compared to the mirror image voxels on the white matter of the normal contralateral hemisphere. Spectral post-processing was performed using the software provided by the MRI system manufacturer (Siemens Syngo, VB 15, Siemens Medical Solutions, Erlangen, Germany).

Imaging Findings

For 11 years, repeated 1.5T MRI examinations revealed a slowly growing, non-enhancing tumor mass in the left cerebellar hemisphere with preservation of the gyral pattern. Thus, the present study was done without administration of contrast media. On MRI at 1.5T and 7T, the posterior fossa tumor ($49 \times 34 \times 32$ mm in size) appeared mainly hyperintense on the T2-weighted images (Fig. 1A) and iso-hypointense on the proton density images (not shown). The characteristic striated pattern of the lesion was best displayed on the T2-weighted images at both field strengths (Fig. 1A, B). The tumor caused descensus of the cerebellar tonsils, but any obstructive supratentorial hydrocephalus was absent. Due to their high sensitivity for paramagnetic substances like deoxyhemoglobin, the SWI and T2* weighted images revealed thin veins running deep between the thickened folia of the cerebellar lesion in great detail (Fig. 1C–F). The 7T SWI minimal intensity projection (MIP) images depicted thin vessel branches as small as 250 μm, whereas the 1.5T SWI MIP images could only resolve larger vessels to a size of 450 μm. Compared to the 1.5T SWI images (Fig. 1C) the medial displacement and compression of the dentate nucleus by the tumor were much better registered on 7T SWI images (Fig. 1D). The ^{1}H-MRS at 1.5T demonstrated a reduction in NAA and a prominent lactate peak. Contrary to other previous reports, the Cho, Cr and the resulting Cho/Cr ratio were slightly elevated in the lesion and the myoinositol (MI) levels were not changed (3, 4). Thus far, neurosurgical therapy and histopathological examination have not been performed because the lesion exerted only mild compression of the IV ventricle without any hydrocephalus.

A DNA analysis revealed a heterozygous mutation in exon 5 of the *PTEN* gene (chromosome 10 q23), and this supported the diagnosis of LDD (c. 388C > T; p. Arg130X). The patient received genetic counseling and is under neurological review.

DISCUSSION

Lhermitte-Duclos disease or dysplastic cerebellar gangliocytoma is a slowly enlarging mass within the cerebellar cortex, and patients with this malady present with headaches, occlusive hydrocephalus, cranial nerve palsies, gait ataxia and other symptoms of cerebellar dysfunction (1). Beside some pediatric cases, the majority of patients are diagnosed in the third or fourth decade of life without a gender predilection. Histopathologically, LDD is characterized by regional enlargement of the cerebellar stratum granulosum, an absence of the Purkinje cell layer and progressive hypertrophy of the granular cell neurons with increased myelination of their axons in the

Table 1. MRI Sequence Parameters Used at 1.5T and 7T

Parameter	1.5T PD/T2	7T PD/T2	1.5T SWI	7T SWI	1.5T T2*	7T T2*
Repetition time (msec)	4000	6000	49	27	700	650
Echo time (msec)	14/81	11/95	40	15	26	18.1
Flip angle (°)	150	130	15	15	20	30
Bandwidth (Hz/pixel)	106	257	80	160	80	40
Acquisition matrix (pixel)	512*256	512*512	256*202	512*512	256*192	1,024*1,024
Voxel volume (mm^3)	0.9/0.4/1.0	0.5/0.5/2.0	1.1/0.9/2.0	0.5/0.5/3.0	1.2/0.9/6.0	0.3/0.3/3.0
Slices	24	10	80	88	20	18
Parallel acquisition (R = 2)	GRAPPA	GRAPPA	GRAPPA	GRAPPA	none	GRAPPA
Acquisition time (min: sec)	2: 46	4: 24	4: 41	7: 26	3: 40	4: 46

Note.— PD = proton density, SWI = susceptibility weighted images, GRAPPA = generalized autocalibrating partially parallel acquisition

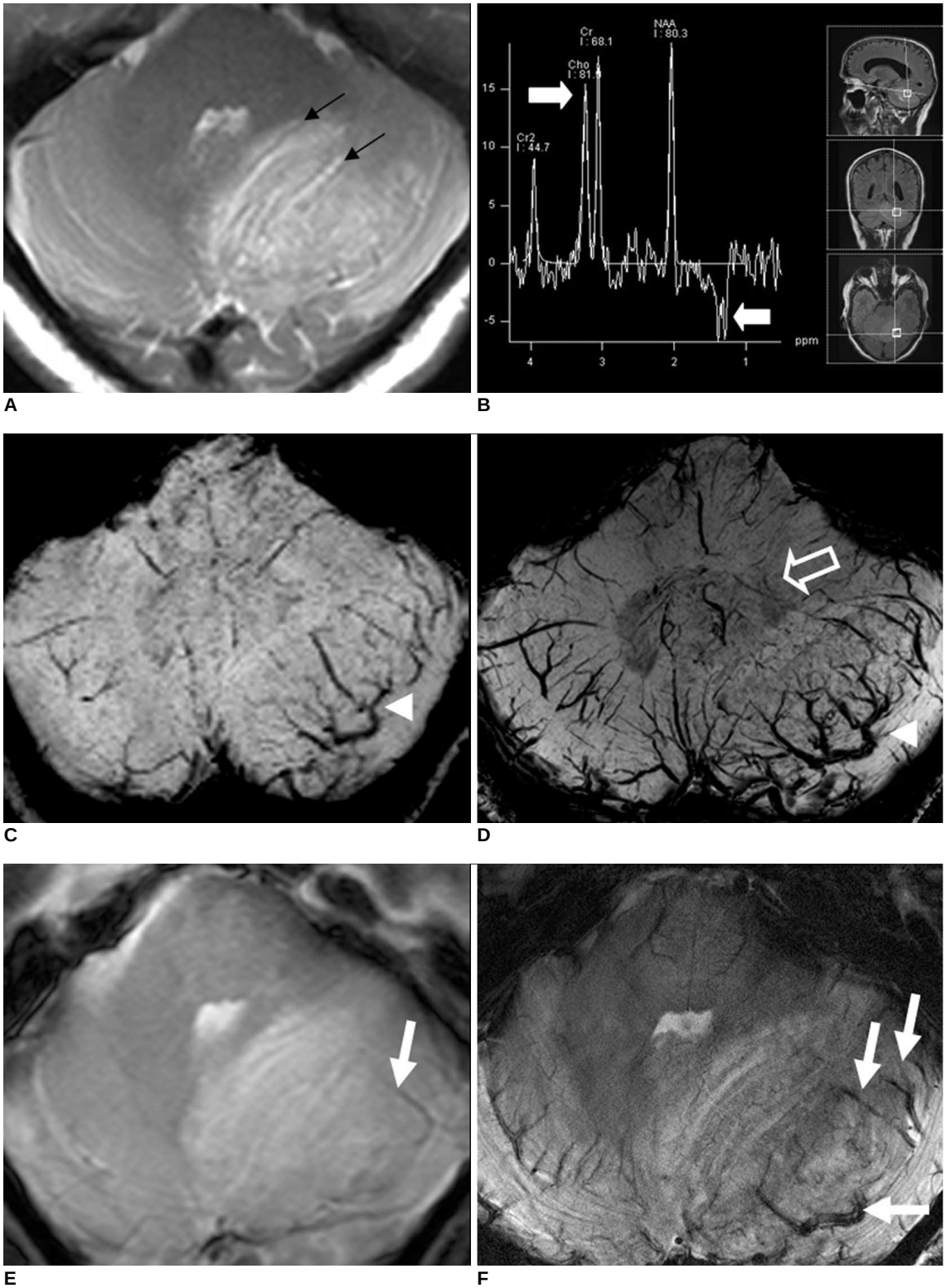

Fig. 1. Dysplastic cerebellar gangliocytoma in 46-year-old man.
A. 1.5T T2-weighted axial image reveals left cerebellar mass with typical 'tiger striped' pattern of alternating inner hyperintense and outer hypointense layers (black arrows).
B. Proton-MR spectroscopy (TE 135 ms) shows inverted lactate peak and reduction in choline (white arrows).
C, D. 1.5T susceptibility weighted minimal intensity projection image depicts single veins running deep between thick folia (arrowheads), whereas 7T susceptibility weighted image demonstrates compression of dentate nucleus (open arrow in **D**) and multiple, draining veins in greater detail.
E, F. Due to increased sensitivity for susceptibility effects, 7T T2* weighted image (**F**) shows more peritumoral veins (white arrows) than corresponding 1.5T T2* image (**E**).

expanded molecular layer (5).

MRI has proven to be the best imaging modality for revealing the characteristic appearance of LDD, and MRI often enables physicians to make the diagnosis of LDD even without histopathological confirmation (3, 4, 6–10). The striated pattern of LDD is a result of the close apposition of the thickened cerebellar folia that are lacking their secondary arborization. A non-enhancing, unilateral cerebellar mass in a middle-aged patient, which is characterized by a 'tiger-striped' pattern of hyperintensity on the T2-weighted MR images and this respects the cerebellar margins, is typical of LDD (8). To the best of our knowledge, this is the first reported case of LDD that has been examined by 7T MRI ultrahigh field MRI systems ($\geq$ 7T) with their increased signal-to-noise ratio (SNR) and higher sensitivity to susceptibility contrast. These systems are currently being tested for clinical applications and they allow for imaging anatomical structures with thinner sections, larger matrices and reduced acquisition times. However, the clinical challenges associated with 7T MRI include higher specific absorption rates (SAR), non-uniformity of the transmitted radiofrequency field, non-homogeneity of the static magnetic field, increased susceptibility artifacts and potential physiological side-effects. Moving from 1.5T to 7T MRI, the T2* is shortened and the susceptibility contrast of paramagnetic substances (e.g. deoxyhemoglobin, neuromelanin, iron) is significantly amplified, which enables a superior illustration of the venous vasculature and cerebellar nuclei. 1.5T SWI was found to be helpful for detecting deep running veins around the thickened folia of LDD (3). 7T SWI can demonstrate in greater detail veins that are even smaller than the voxel size, due to the associated paramagnetic effect, than the corresponding 1.5T images (Fig. 1C–F) because the sensitivity of MRI scanners for paramagnetic substances increases in proportion to the applied magnetic field. The deoxyhemoglobin in these veins helps to resolve the outer most layer of the LDD, which consists of the outer molecular layer, the leptomeninges and the associated abnormal vessels. Thomas et al. (3) and Kulkantrakorn et al. (7) reported good correlation of this MRI pattern with the histological specimen. Beside the characteristic striated pattern on the T2-weighted images, these abnormal veins surrounding the thickened folia on the SWI images seem to be another unique feature of LDD. Beside the preoperative identification of LDD, the higher resolution of 7T SWI may help to depict large draining veins and the cerebellar nuclei. Their anatomical relation is of clinical importance for planning surgical procedures because lesions affecting the cerebellar nuclei are associated with more severe symptoms than are cortical lesions. ^{1}H-MRS demonstrated a prominent lactate peak, suggesting increased glycolysis and the high metabolism of this LDD lesion (4, 9). Decreased levels of Cho, Cr, NAA and MI and the Chr/Cr are normally found on the side affected by the LDD (9). The slightly increased Cho levels in our patient suggested increased demyelination and membrane turnover, whereas the decreased Cho levels in the lesion suggested a non-neoplastic etiology of this lesion (4, 9).

Making the preoperative diagnosis of LDD via MRI obviates the need for biopsy and this allows surgeons to plan an appropriate therapy, which consists of decompression of the posterior fossa by total surgical resection. Tumor resection has not yet been performed in our patient due to the mild clinical symptoms.

In conclusion, as seen on MRI, a non-enhancing, 'tigers striped' cerebellar lesion with unilateral hemispheric expansion and preservation of the gyral pattern should be considered specific for LDD and these findings often allow making the preoperative diagnosis. 7T MRI more precisely reveals the known morphology and microstructure of this tumor entity than can 1.5T MRI. Especially, 7T SWI enables the identification of the outermost layer of LDD due to its inherent venous vasculature, and 7T SWI better displays the iron containing dentate nuclei. Hence, 7T MRI is expected to become a valuable tool for studying the cerebral microvascularity and tumor angiogenesis not only for LDD, but also for other resectable brain tumors.

Acknowledgement

The authors thank Dr. B. Albrecht for contributing all the results of the genetic analysis.

References

1. Lhermitte J, Duclos P. Sur un ganglioneurome diffuse du cortex du cervelet. Bulletin de l' Association francaise pour l' etude du cancer. *Paris* 1920;9:99-107
2. Padberg GW, Schot JD, Vielvoye GJ, Bots GT, de Beer FC. Lhermitte-Duclos disease and Cowden disease: a single phakomatosis. *Ann Neurol* 1991;29:517-523
3. Thomas B, Krishnamoorthy T, Radhakrishnan VV, Kesavadas C. Advanced MR imaging in Lhermitte-Duclos disease: moving closer to pathology and pathophysiology. *Neuroradiology* 2007;49:733-738
4. Klisch J, Juengling F, Spreer J, Koch D, Thiel T, Buchert M, et al. Lhermitte-Duclos disease: assessment with MR imaging, positron emission tomography, single-photon emission CT, and MR spectroscopy. *AJNR Am J Neuroradiol* 2001;22:824-830
5. Ambler M, Pogacar S, Sidman R. Lhermitte-Duclos disease (granule cell hypertrophy of the cerebellum) pathological analysis of the first familial cases. *J Neuropathol Exp Neurol* 1969;28:622-647
6. Carter JE, Merren MD, Swann KW. Preoperative diagnosis of Lhermitte-Duclos disease by magnetic resonance imaging. Case

report. *J Neurosurg* 1989;70:135-137
7. Kulkantrakorn K, Awwad EE, Levy B, Selhorst JB, Cole HO, Leake D, et al. MRI in Lhermitte-Duclos disease. *Neurology* 1997;48:725-731
8. Meltzer CC, Smirniotopoulos JG, Jones RV. The striated cerebellum: an MR imaging sign in Lhermitte-Duclos disease (dysplastic gangliocytoma). *Radiology* 1995;194:699-703
9. Nagaraja S, Powell T, Griffiths PD, Wilkinson ID. MR imaging and spectroscopy in Lhermitte-Duclos disease. *Neuroradiology* 2004;46:355-358
10. Wolansky LJ, Malantic GP, Heary R, Maniker AH, Lee HJ, Sharer LR, et al. Preoperative MRI diagnosis of Lhermitte-Duclos disease: case report with associated enlarged vessel and syrinx. *Surg Neurol* 1996;45:470-475